

## STUDY OF SURFACE MORPHOLOGY OF WSe<sub>2</sub> SINGLE CRYSTAL BY ATOMIC FORCE MICROSCOPY

C. A. Patel<sup>1</sup> and Kaushik R. Patel<sup>2\*</sup>

<sup>1</sup>Pilvai Science College, Pilvai (Gujarat)

<sup>2</sup>Biogas Research and Microbiology Department, Gujarat Vidyapith, Ahmedabad

\*Author for Correspondence: [krpatel@gujaratvidyapith.org](mailto:krpatel@gujaratvidyapith.org)

### ABSTRACT

The single crystals of tungsten diselenide were grown by direct vapour transport (DVT) technique. The stoichiometry of as grown crystals was confirmed with the help of Energy Dispersive Analysis by X-ray (EDAX). The Surface morphology of as grown crystals was studied by atomic force microscopy. It gives 2D and 3D images, height profiles, power spectral density curves, histogram curves, bearing ratio curve and surface parameter. These data provides information about the roughness/smoothness of the sample. The results obtained are discussed in detail.

**Keywords:** Single Crystals, EDAX, XRD, Surface Morphology, AFM

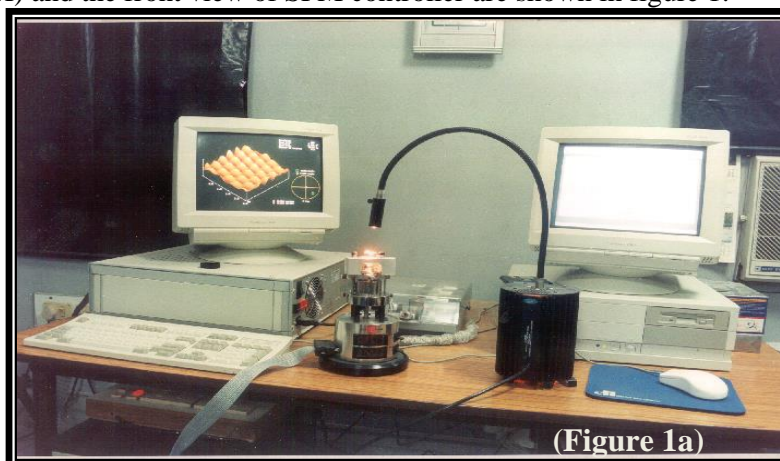
### INTRODUCTION

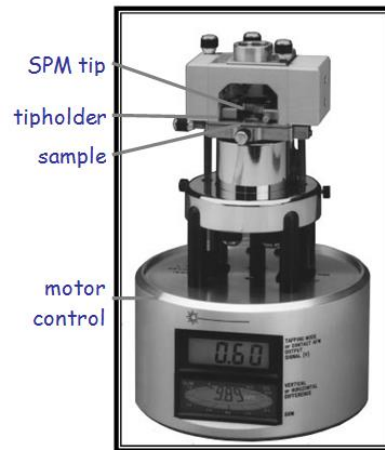
The optical properties of TMDCs were first explained in terms of their electronic bands by Wilson and Yoffe [1]. The tungsten diselenides (WSe<sub>2</sub>), a member of II-VI group has regular layered structure with six-fold trigonal prismatic coordination of the metal atoms by the chalcogen atoms (X-M-X) within the layers.

The structural parameters, Deformation and Growth fault probability and surface morphology of as grown crystals of WSe<sub>2</sub> were studied by Patel *et al.*, [2]. AFM is one type of scanning probe microscope, which has an ability to create three dimensional micrograph of sample surface with resolution down to the nano-meter and angstrom scale. The AFM is one of the foremost tools for imaging, measuring and manipulating matter at the nanoscale. AFM is also known as scanning force microscope (SFM) because by using AFM one can image the surface with atomic scale resolution and at the same time one can also measure the force at nano-scale. This force is between the tip and the sample surface like Van der Waal force with resolution in the range of few nano-newtons.

### MATERIALS AND METHODS

The EDAX of the grown WSe<sub>2</sub> single crystals in the present investigation was carried out using the electron microscope (Make: Phillips, Model: XL 30 ESEM). The Photographic view of Atomic Force Microscope (AFM) and the front view of SPM controller are shown in figure 1.





(b)

**Figure 1:** Atomic Force Microscope (AFM) (a) Photographic view (b) front view of scanning probe microscope (SPM).

## 2.1 Background / Surface Roughness Parameters and Statistical Measures With AFM

The atomic force microscope (AFM) is not only an excellent tool for recording the surface topography of a sample, but also proven to be a good means for studying the strength of chemical bonds [3,4], the elastic and mechanical properties of macromolecules [5-8] and the intermolecular interactions at the single molecular level [9-11].

The AFM instrument produces three-dimensional images of the surface. Though AFM images are often used as micrographs of the surface, the data are also used to measure another important parameter such as surface roughness. Surface roughness influences/causes as wear [12] and light scattering from the surfaces [13-14]. In semiconductor manufacturing, roughness of bare Silicon wafers is measured after polishing and cleaning. Excessive roughness destroys the integrity of very thin layers, such as gate or tunnel oxide. Roughness is equally important for other electronic materials, such as SiC (silicon carbide) and GaAs (gallium arsenide). In optics, surface roughness causes light scattering, which can be good or bad for the product, depending on the application. For high quality X-ray mirrors, both the substrate roughness and the coating roughness are measured and must be minimized. For diffusers, controlled roughness is important to achieve the desired effect; part of its control is related to the roughness power spectrum, so that the diffused scattering is isotropic and achromatic. In the paper industry, surface roughness and porosity are critical factors in determining whether a paper can sell for \$1/sheet (photo quality inkjet paper), \$0.005/sheet (multipurpose photocopier paper), or somewhere in the middle. In general, the AFM demonstrates subtle, yet important, effects of surface treatment, corrosion and aging in a wide variety of materials, including metals, ceramics, glasses, semiconductors and polymers.

The AFM system can also draw surface profiles in any traverse direction and of any traverse length within the original area scan, together with the power spectrum, the height histogram, the bearing ratio and the selected surface parameters for each chosen traverse length [15]. Various statistical quantities such as average, peak-to-valley and root-mean-square roughness have been obtained to characterize surface topography. However, they provide only vertical information. Since the spectral analysis provides both lateral and longitudinal information, it is a more informative measurement than all the above mentioned commonly used statistical quantities.

## 2.2 One-Dimensional Surface Roughness Parameters (Roughness Amplitude Parameters)

Surface roughness can be quantified using a variety of different parameters [13] that can be divided into two groups. (1) Single values to describe the roughness and (2) statistical measures of the roughness. Two common single value parameters for roughness are the arithmetic roughness ( $R_a$ ) and the rms roughness ( $R_{rms}$ ). Unfortunately, these two parameters only describe the vertical roughness of a surface.

**Research Article (Open Access)**

Two surfaces with identical vertical roughness can have very different surface morphology [16,17], and a measure of the horizontal roughness is needed to accurately specify their roughness distinctly [13]. Statistical measures of surface roughness provide a more complete description of the surface than single valued parameters [12]. Two commonly used statistical measures of surface roughness are the bearing ratio and the power spectral density (PSD). The bearing ratio is a useful parameter for characterizing abrasive wear of the surfaces [12] and the PSD is the power spectrum of the Fourier transform of the surface profile [12] which provides useful information on the geometrical structure of the surface. In particular, it is useful for detecting periodic structure in the profile. The meanings of all such parameters are discussed below.

**2.3 Roughness Average /Arithmetic Roughness  $R_A$**

In general, the roughness average can be considered as the arithmetical mean deviation of all the points or it can be defined as the average deviation of roughness of all points in the profile from a mean line over the evaluation length [18]. The arithmetic roughness  $R_a$  of a surface can be expressed as

$$R_a = \frac{1}{N} \sum_{j=1}^N |r_j| \tag{1}$$

where N is the number of data points of the profile and

$$r_j = z_j - \bar{z}$$

where  $z_j$  are the data points that describe the relative vertical height  $z_j$  of the surface and  $\bar{z}$  is the mean height of the surface given by the equation

$$\bar{z} = \frac{1}{N} \sum_{j=1}^N z_j \tag{2}$$

**2.4 Root Mean Square Roughness  $R_Q$**

Root mean square roughness is defined as “The average of the measured height deviations taken within the evaluation length and length measured from the mean line” [19]. It can be mathematically expressed as

$$R_q = \sqrt{\frac{1}{N} \sum_{j=1}^N r_j^2} \tag{3}$$

**2.5 Maximum Profile Peak Height  $R_p$**

It is defined as “the height of the maximum/highest high intensity peaks in the roughness profile over the evaluation length”[18]. The maximum profile peak height is represented mathematically as

$$R_p = \left| \max_{1 \leq j \leq N} r_j \right| \tag{4}$$

**2.6 Maximum Profile Valley Depth  $R_v$  or  $R_M$**

It is defined as “the depth of the deepest valley in the roughness profile over the evaluation length” [18] which may be given mathematically as

$$R_v = \left| \min_{1 \leq j \leq N} r_j \right| \tag{5}$$

**2.7 Maximum Height of The Profile  $R_T$  or  $R_{p-v}$**

Maximum height of the profile basically is a measure of the maximum peak to valley height in the roughness profile. The exact definition of it may be given as “The absolute value between the highest and lowest peaks”[19]. The mathematical expression used to calculate the parameter is

$$R_t = \left| \min_{1 \leq j \leq N} r_j \right| + \left| \max_{1 \leq j \leq N} r_j \right| \quad (6)$$

### 2.8 The Amplitude Distribution Function (ADF)

The amplitude distribution function is a probability function that gives the probability that a profile of the surface has a certain height  $z$  at any position  $x$  [20].

### 2.9 The Bearing Ratio Curve (BRC)

The Bearing Ratio Curve is related to the ADF. It is the corresponding cumulative probability distribution. The bearing ratio curve is always integral (from the top down) of the ADF [20]. The bearing ratio ( $t_b$ ) is defined as the length of the profile above a horizontal line through the distribution [12] and is typically shown as a graph in which the ordinate is the height below the highest peak in the profile. This makes the bearing ratio curve more accurate reflection of the vertical roughness of the surface than arithmetic or RMS roughness. The length of the surface is a measure of the vertical roughness of the surface (of the crystal) whereas the shape of the bearing ratio curve is an indication of the topography of the surface [21]. It finds much greater use in evaluating surface finish.

### 2.10 Power Spectrum

The most important property of rough surfaces is the surface roughness power spectrum. It determines the contact area between two solids and can provide both lateral and longitudinal informations. Thus it is more informative measurement than all the statistical quantities.

Surface roughness is often understood as a departure of the roughness parameters from the planarity. A convenient way of describing surface roughness is to represent it in terms of profile height  $z(x, y)$ . For typical digitized AFM scans, the values of  $x$  and  $y$  are quantized. To determine PSD, one needs to transform 2D AFM images from real space to reciprocal space. Two types of Transformations are used by various authors: one is the Fast Hartley transform (FHT) [16] and the other is the Fast Fourier transform (FFT) [22-28].

Even though the 2D FFT and FHT give us a transformed version of the reciprocal space, it is still difficult to make use of this 2D information. The standard method to solve this problem is to extract a 1D magnitude of the 2D transform; that is, a 1D power spectral density is plotted against the spatial frequency. For a typical 2D AFM Scan, it consists of 250 000 (i.e.  $512 \times 512$ ) data points, but the 1D PSD requires 512 pieces of information to describe the surface roughness. This method was proposed independently by Dumas et al. [23] and Strausser et al. [24, 29].

In AFM, one and two-dimensional power spectral density (PSD) are used to characterize the structure of the surfaces. In the present work, (1D) PSD is considered, as the simulations used are line scans and not two dimensional images. The 1D PSD is given by the relation [30],

$$PSD_{1D} = \frac{1}{L} \left( \frac{\pi}{2} \int y(x) e^{i(px)} dx \right)^2 \quad (7)$$

where  $L$  is the length of the profile and  $y(x)$  is the profile.

The power spectral density is advantageous because it allows comparison of the roughness data taken over various spatial frequency regions. Such methodology also offers a convenient representation of the direct space periodicity and amplitude of the roughness.

## RESULTS AND DISCUSSION

The  $WSe_2$  single crystals were successfully grown by direct vapour transport technique. From EDAX analysis the grown crystals are stoichiometrically perfect without any other impurities.

The as-grown single crystals of  $WSe_2$  were viewed under the non-contact AFM mode. Silicon nitride tip was used to obtain topographic images of surfaces of the single crystals. One can also obtain various line analyses spectrums from real images by the Digital Instruments 2SPM controller using di CP-II ProScan 1.9 software.

**Research Article (Open Access)**

Figure 2 (a and b) shows the 2D and 3D AFM images covering an area of  $2\mu\text{m} \times 2\mu\text{m}$  of  $\text{WSe}_2$  crystals. The images are computer generated and the original data can be manipulated so that the surface of interest can be viewed from different directions. Distance scales in the x, y and z directions are marked on the 3D images and the z scale can be exaggerated as required.

The 3D images (maximum  $256 \times 256$  points) do facilitate over all visualization of the crystal surface. An image in a 3D format gives a rendition of what the surface topography actually looks like. That is, the data is displayed in the x y and z axis. Often the scale between the x, y and z axis are not equal. The surface features are very small with relationship to the x and y dimensions; however, in 3D image they look large. This figure reflects that the surface possesses hilly (also valley) regions and is not absolutely flat surface [30].

The two dimensional image shows the x and y axis and color is used to depict the height of image. An AFM image displayed in the 2D format looks much like an image obtained from a traditional microscope such as an optical microscope. Dark area starting from LHS of the figure on the top and turning and terminating at the bottom probably belongs to a part of the hexagonal spiral step in the optical image.

To know the surface morphology of  $\text{WSe}_2$  single crystals, the line analysis is carried out in detail. The line profile is a two dimensional profile or cross section extracted from an AFM image. This may be taken horizontally, vertically or at obtuse angles. The results of line analysis for  $\text{WSe}_2$  single crystal is given in table 1. A line trace of the surface profile along the chosen traverse length can be printed out together with the height profile, histogram, power spectrum, bearing ratio along with various statistical parameters as already mentioned earlier (table 1). The line-1 to 8 (shown in fig. 3.2(a)) have drawn on the surface of the crystal show indirectly the typical arrangement of the growth features in those regions. The height profiles taken along the horizontal and vertical line 1 to 8 of the AFM image of  $\text{WSe}_2$  single crystal is shown in figure 3 (1 to 8). This reveals the fact that the difference between the peak p and the valley z or v values ( $R_p-v$ ) have been found to be in the range 2nm and 11nm of line-1 to line - 8, indicating crystal at location of line 5 has almost double maximum peak to valley difference than at location of line - 3. The rms and  $R_a$  roughness values for line-1 are found to be 1.679nm and 0.8298nm respectively, whereas for line-3 these values are 0.3922nm and 0.2576nm respectively, indicating that there is no significant difference in average and rms values of peaks across these lines. It may be noted that these parameters indicate roughness in vertical direction. Bearing ratio of line-1 to line-8 is suggesting horizontal roughness shown in figure 6 (1 to 8).

The region chosen for line-5 is more smooth/uniform as compared to that of another line. Furthermore, the arrangement of atoms as revealed in 3D image shows peaks and valleys. This type of arrangement of atoms is uniform from 2nm to 11nm and is depicted in 3D image of the same crystal. However these two single value parameters (i.e  $R_{\text{rms}}$  and  $R_a$ ), though simple and reliable, make no distinction between peaks and valleys and do not account for the lateral distribution of surface features. A more complete description is provided by the Power Spectral Density (PSD) calculations of the surface topography, which perform a decomposition of the surface profile into its related spatial wavelengths and allows comparison of the roughness measurements over different spatial frequency ranges [31]. Thus, the variation of height fluctuations can be represented more accurately through the Power Spectral Density (PSD). This quantity can be calculated by performing a Fourier transform of the 2D height data [32, 33]. The Fourier conjugate variable is the spatial frequency which corresponds to the lateral feature sizes, while the strength of the distribution at each spatial frequency corresponds to average height information for those feature sizes.

The power spectral density curves corresponding to line 1 to line - 8 are shown in figure 4 (1 to 8). All these curves have the same general shape, which indicates that the overall surface of  $\text{WSe}_2$  single crystal is homogeneous. However, a number of peaks consists more at lower frequency, corresponding to the large features in the image. Also, the position of the peaks in the PSD curves at low spatial frequencies varies with lines (figure 3.4,1 to 8). At higher spatial frequencies the amplitude of the PSD curves gradually decreases. These PSD curves also provide information across the entire frequency range of the scanned surface ( $2\mu\text{m} \times 2\mu\text{m}$ ) including waviness (mid frequency) and form (lower frequency). The peaks in the PSD indicate the periodicity of the surface. The frequency of each peak gives the length that

**Research Article (Open Access)**

defines this periodic surface and the spread in the peak indicates the magnitude of the deviation from the average value.

The Mean height indicates the central value in the roughness profile over the evaluation length and is found to be 7.50nm, while median height is a mid point on the roughness profile over the evaluation length such that half of the data fall above it and half below it which turns out to be 7.35 nm. The horizontal measurement of roughness  $n(0)$  can be studied from height profile (figure 3, 1 to 8), which indicates the number of intersections that the profile makes with the mean line of the profile over a specified distance.

The height distributions (Histograms) obtained from 2D AFM image of  $WSe_2$  crystals are shown in figure 5 (1 to 8). The histogram is a continuous bar diagram in which each column represents a height range. The height of each column represents the number of image pixels which have a height value in a particular range. The histogram of height distributions in figure 3.5 (1 to 8) shows that most of the corrugation heights on  $WSe_2$  single crystal surface lie between 9 nm to 10 nm above the lowest point within the given area. Also, polygon can be prepared by joining the mid points of the bars. The histogram and polygon considered together indicate that the height distribution is asymmetric. That is the distribution for all histograms is positively skewed, as mean values for all lines are greater than the median value except line 3, 6 and 8.

The bearing ratio from the 2D AFM image for eight different lines was measured at 80% or above 6.07nm for line-H<sub>4</sub> and 7.64 nm for line-V<sub>6</sub> from the lowest point.

**Table 1:** Surface parameters as obtained from the AFM profiles of  $WSe_2$ .

Line No.	R <sub>P-V</sub> (nm)	Rms Rough (Rq) (nm)	Ave Rough (Ra) (nm)	Mean Ht (nm)	Median Ht (nm)	Arc length (μm)	Bearing Ratio @30% (nm)	Bearing Ratio @80% (nm)	Peak (R <sub>P</sub> ) (nm)	Valley (R <sub>V</sub> ) (nm)
H-1	8.734	1.679	0.8298	7.555	7.160	2.014	7.52	6.92	6.762	-1.972
H-2	2.669	0.6855	0.6268	7.551	7.157	2.010	8.25	6.91	1.426	-1.243
H-3	2.183	0.3922	0.2576	7.562	7.642	2.010	7.76	7.52	0.564	-1.619
H-4	3.760	1.322	1.219	7.530	7.158	2.010	8.86	6.07	1.933	-1.828
V-5	10.56	0.8910	0.5550	8.004	7.888	2.019	8.25	7.40	6.191	-4.364
V-6	6.189	0.4449	0.3320	7.969	8.006	2.015	8.13	7.64	4.650	-1.539
V-7	9.952	1.394	0.6514	8.012	7.763	2.038	7.89	7.40	8.885	-1.097
V-8	4.969	0.5387	0.4064	7.098	7.157	2.014	7.40	6.67	3.577	-1.392

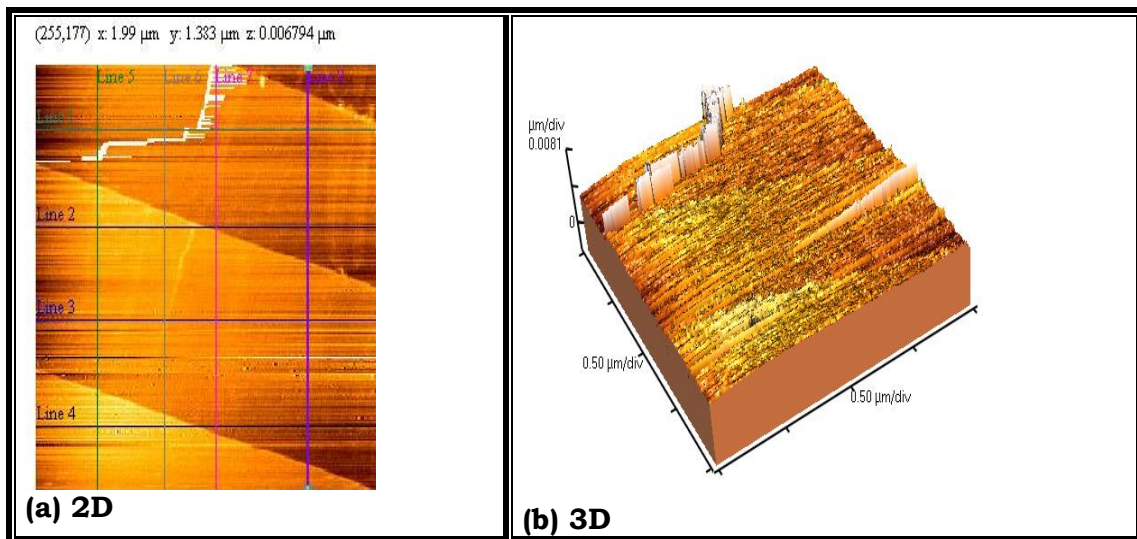


**Figure 2:** (a) 2D and (b) 3D, AFM image of  $WSe_2$  single crystals

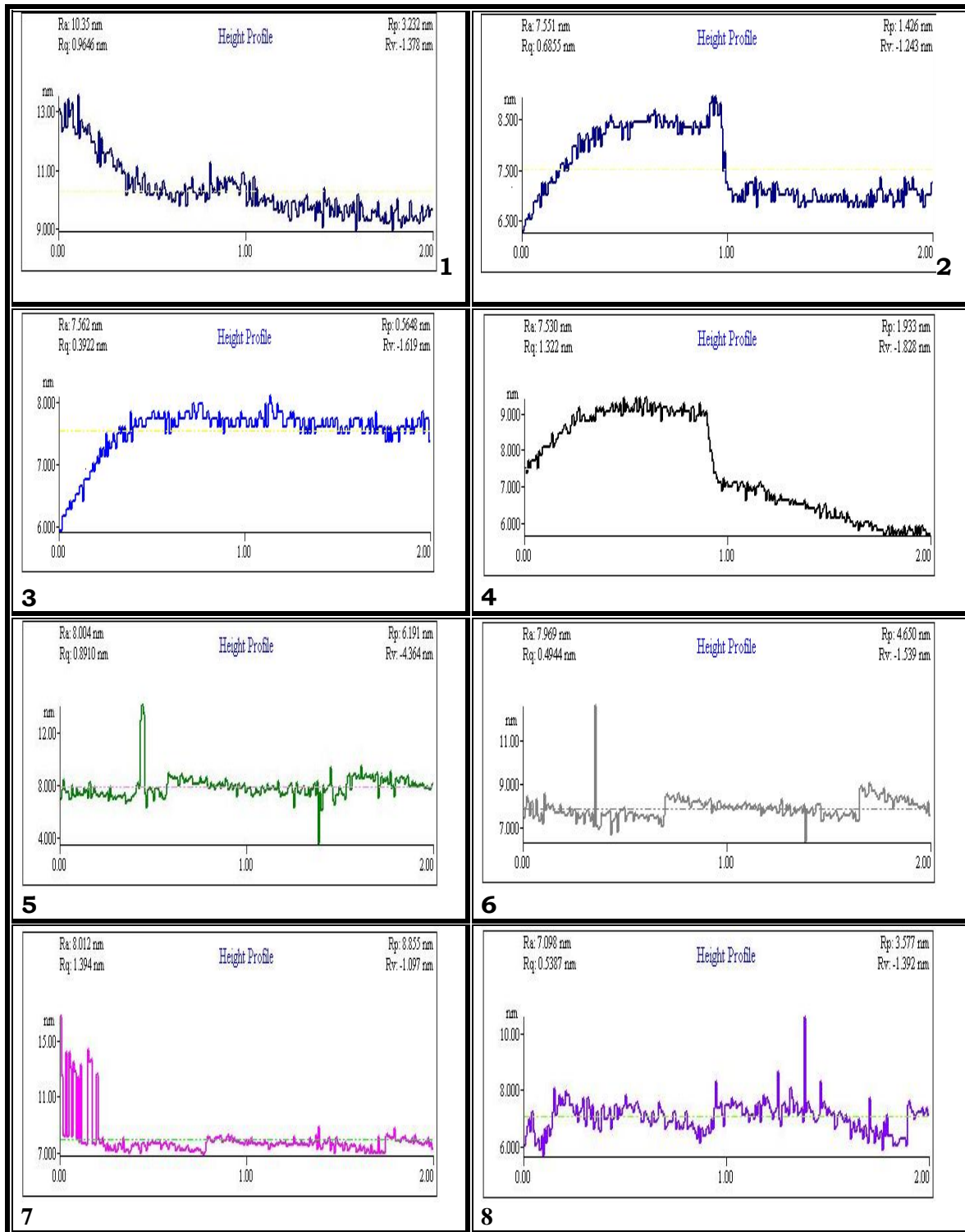


**Figure 3 (1 to 8):** AFM height profiles at various positions of the surface of WSe<sub>2</sub> single crystal.



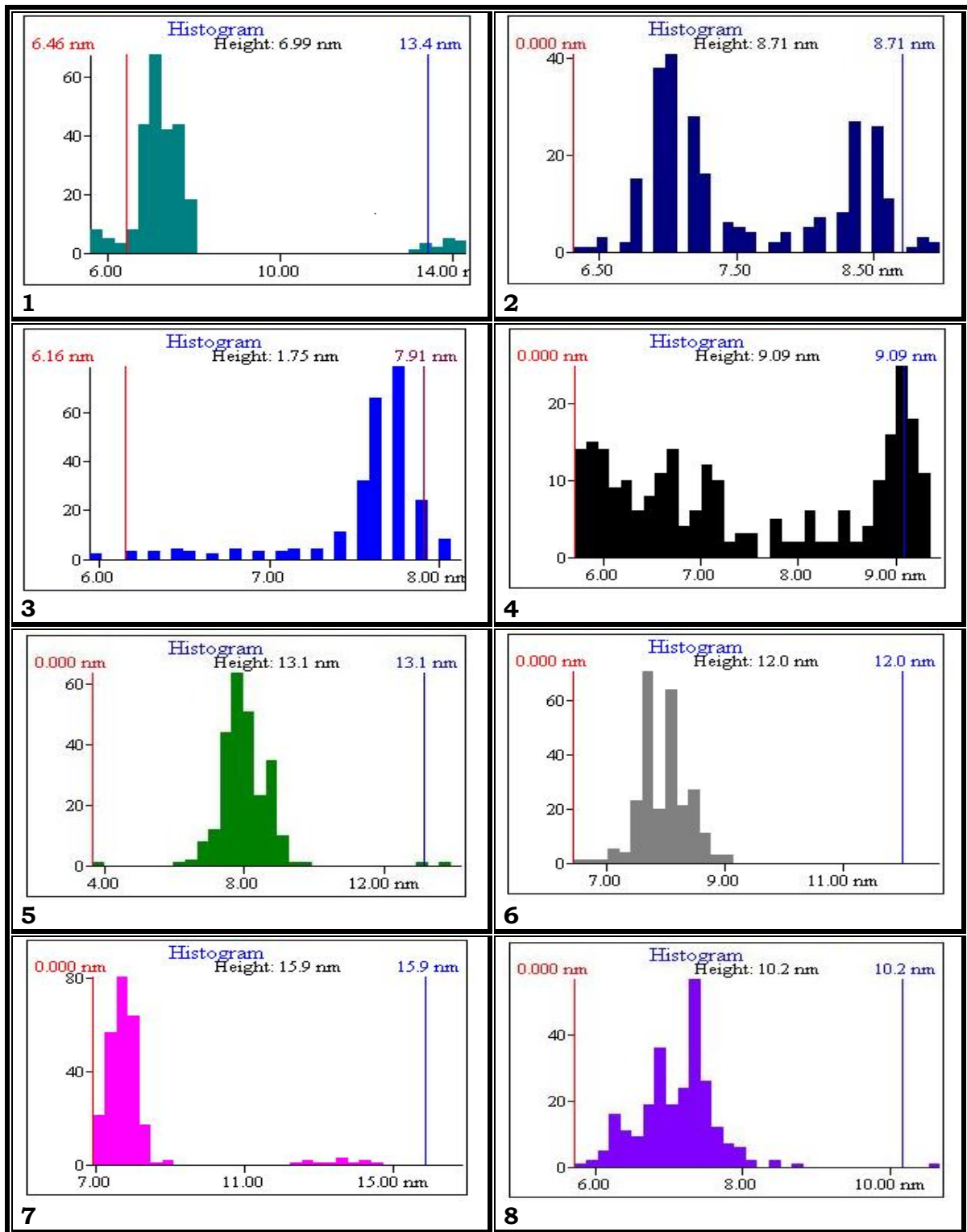


**Figure 5 (1 to 8):** The Histogram curves at various positions of the surface of WSe<sub>2</sub> single crystals.

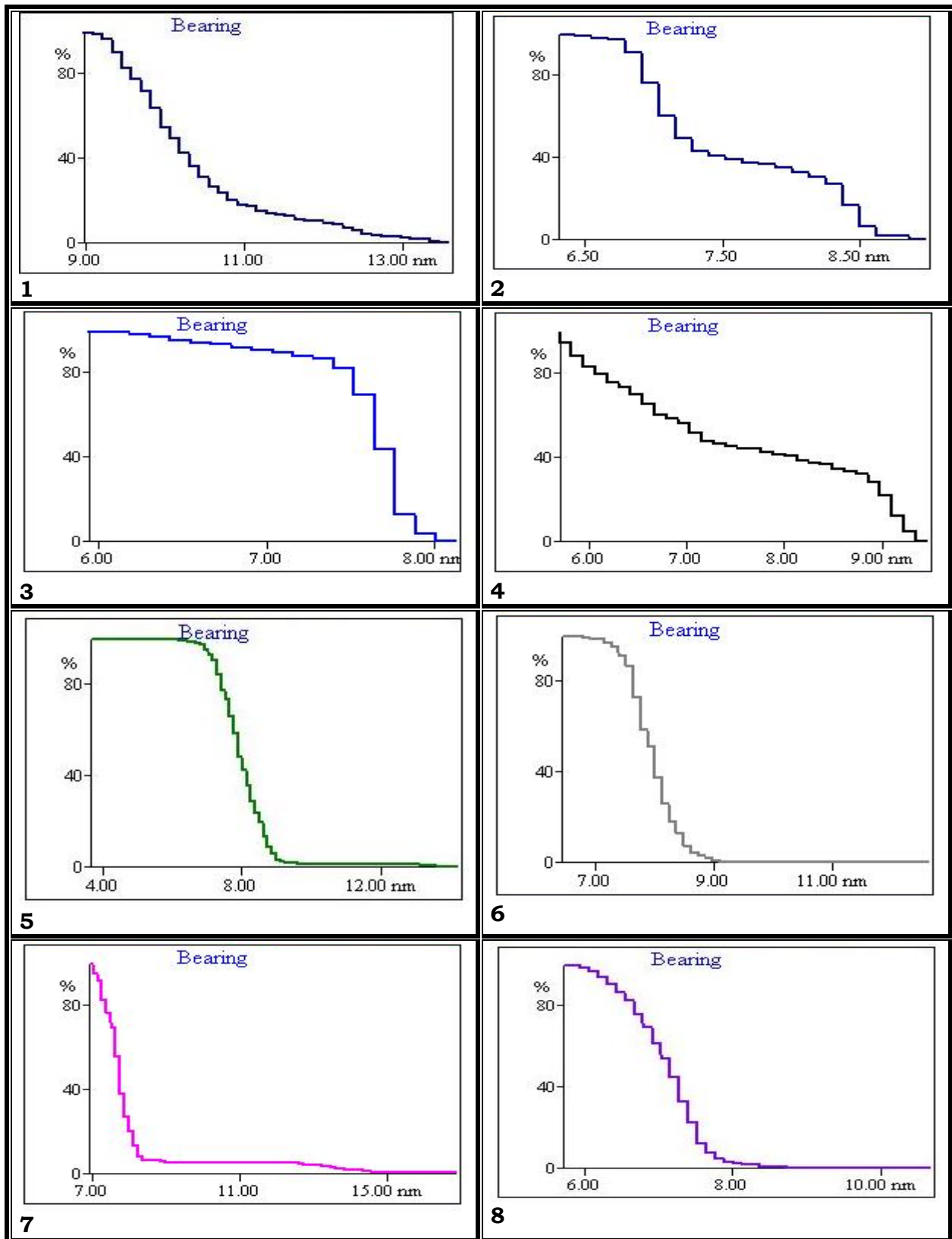


**Figure 6 (1 to 8):** The Bearing ratio curve at various positions of the surface of WSe<sub>2</sub> single crystal.

## CONCLUSION

WSe<sub>2</sub> crystals were grown by direct vapour transport technique and the stoichiometry of as grown crystal was confirmed by EDAX. Surface study by atomic force microscopy gives 2D and 3D images, height profiles, power spectral density curves, histogram curves, bearing ratio curve and surface parameter of as grown crystal of WSe<sub>2</sub> for different sample of as grown WSe<sub>2</sub> single crystals. Finally with the help of these data one can say about the roughness/smoothness of the sample.

## REFERENCES

- [1] **Wilson J A, Yoffe A D**, “The transition metal dichalcogenides discussion and interpretation of the observed optical, electrical and structural properties” *Adv. Phys.*, **18** (1969) 193
- [2] **CA Patel, Kaushik R Patel and KD Pate**, “Structural characterization of tungsten diselenide single crystal” *International Journal of Physics and Mathematical Sciences*, 2012 Vol. 2 (4) pp.17-26
- [3] **Frisbie C D, Rozsbyai L F, Noy A, Wrighton M S, Lieber C M**, “Functional group imaging by chemical force microscopy” *Science* **265** (1994) 2071
- [4] **Grandbois M, Rief M, Clausen–Shaumann H, Gaub H E**, “How Strong Is a Covalent Bond?” *Science* **283** (1999) 1730
- [5] **Rief M, Oesterhelt F, Heymann B, Gaub H E**, “Single molecule force spectroscopy on polysaccharides by atomic force microscopy” *Science* **275** (1997) 1295
- [6] **Maaloum M, Courvoisier A**, “Elasticity of single polymer chains” *Macromolecules*, **32** (1999) 4989
- [7] **Strunz T, Oroszlan K, Schafer R, Guntherodt H-J**, “Dynamic force spectroscopy of single DNA molecules” *Proc. Natl Acad. Sci. USA*, **96** (1999) 11277
- [8] **Clausen-Schaumann H, Rief M, Tolksdrof C, Gaub H E**, “Mechanical stability of single DNA molecules” *Biophys. J.*, **78** (2000) 1997
- [9] **Florin E L, Moy V T, Gaub H E**, “Adhesion forces between individual ligand-receptor pairs” *Science* **264** (1994) 415
- [10] **Hoh J H, Hillner P E, Hansma P K**, *Proc. Microsc. Soc. Am.*, **52** (1994) 1054
- [11] **Heymann B, Grubmuller H**, “Dynamic force spectroscopy of molecular adhesion bonds” *Phys. Rev. Lett.*, **84** (2000) 6126
- [12] **Gomez S, Hale K, Burrows J, Griffiths B**, “Measurements of surface defects on optical components” *Meas. Sci. Technol.* **9** (1998) 607
- [13] **Nowicki B**, *Wear* **102** (1985) 161
- [14] **Bennett J M, Dancy J H**, “Stylus profiling instrument for measuring statistical properties of smooth optical surfaces” *Appl. Opt.* **20** (1981) 1785
- [15] **Stover J C**, *Optical Scattering, Measurements and Analysis* (McGraw- Hill, New York, 1990)
- [16] **Halepete S D, Lin H C., Fang S J, Helms C R**, “Analyzing Atomic Force Micrographs Using Spectral Methods” *Mater. Res. Soc. Symp. Proc.*, **386** (1995) 383
- [17] **Fang S J, Chen W, Yamanaka T, Helms C R**, “Comparison of Si surface roughness measured by atomic force microscopy and ellipsometry” *Appl. Phys. Lett.*, **68** (1996) 2837
- [18] Standards: ASME B46.1-1995, ASME B46.1-1985, ISO 4287-1997, ISO 4287/1-1997
- [19] Standards: ASME B46.1-1995, ISO 4287-1997
- [20] Standards: ISO 4287-1997
- [21] **Westra K L, Thomson D J**, “Effect of tip shape on surface roughness measurements from atomic force microscopy images of thin films” *J. Vacuum Sci. Technol.* **B13** (2) (1995) 344
- [22] **Helms C R**, in *Semiconductors Characterization: Present Status and Future Needs*, edited by Bullis W M, Seiler D G, Diebold A C (1996), p.110

**Research Article (Open Access)**

- [23] **Dumas Ph, Bouffakhreddine B, Amra C, Vatel O, Andre E, Galindo R, Salvan F**, “Quantitative microroughness analysis down to the nanometer scale” *Europhys. Lett.*, **22** (1993) 717
- [24] **Strausser Y E, Doris B, Diebold A C, Huff H R**,  
Extended Abstract of 185<sup>th</sup> Electrochem. Soc. Meeting, No., **284** (1994) 461
- [25] **Feenstra R M, Lutz M A, Stern F, Ismail K, Mooney P M, LeGoues F K, Stanis C, Chu J O, Meyerson B S**, “Roughness analysis of Si/SiGe heterostructures” *J. Vac. Sci. Technol.* **B13**, (1995) 1608
- [26] **Yoshinobu T, Iwamoto A, Iwasaki,**  
*Jpn. J. Appl. Phys. Part. 1*(33) (1994) L64
- [27] **Bulliks W M**,  
*Micro.*, **14** (1996) 47
- [28] **Courboin D, Grouillet A, Andre E**, “Surface roughness of ion implanted <100> silicon studied by atomic force microscopy” *Surf. Sci.*, **342 (1-3)** (1995) L1111
- [29] **Strausser Y E**,  
Industrial Applications of Scanned Probe Microscopy, National Institute of Standards and Technology, Gaithersburg, MD, March (1994) P.25
- [30] **Shaheen S E, Brabec C J, Serdar Sariciftci N, Pandinger F, Fromherz T, Hummelen J C**, “2.5% efficient organic plastic solar cells” *Appl. Phys. Lett.* **78(6)** (2001) 841
- [31] **Gavrila R, Dinescu A, Mardare D**,  
*Romanian J. Information Sci. Techn.*, **10(3)** (2007) 291
- [32] **Lita A E, Jr Sanchez J E**, “Characterization of surface structure in sputtered Al films: Correlation to microstructure evolution” *J. Appl. Phys.* **85** (1999) 876
- [33] **Buchko C J, Kozloff K M, Martin D C**, “Surface characterization of porous, biocompatible protein polymer thin films” *Biomaterials* **22 (11)** (2001) 1289